*(Article begins on next page)*

# Noise performance of a frequency nondegenerate phase-sensitive amplifier with unequalized inputs

Z. Tong,[1,*] C. Lundström,[1] M. Karlsson,[1] M. Vasilyev,[2] and P. A. Andrekson[1]

[1]Photonics Lab, Department of Microtechnology and Nanoscience, Chalmers University of Technology, Göteborg 412 96, Sweden

[2]Department of Electrical Engineering, University of Texas at Arlington, 416 Yates Street, Arlington, Texas 76019-0016, USA

*Corresponding author: zhi.tong@chalmers.se

Received November 29, 2010; revised January 16, 2011; accepted January 17, 2011; posted February 2, 2011 (Doc. ID 138802); published February 28, 2011

For the first time to our knowledge, the noise performance of a frequency nondegenerate phase-sensitive amplifier (PSA) with unequalized input powers has been experimentally characterized, based on a fiber-based parametric copier-PSA scheme. Two different noise–figure (NF) definitions—separate and combined NFs—are provided and compared. The results show that the separate NF of the weaker input wave is lower than that of the stronger wave due to the correlated-light nature. When considering the combined NF, the optimal noise performance (0 dB NF) is obtained only when the input powers are equal. Experiments agree well with the theoretical predictions. 

*OCIS codes:* 060.2320, 190.4380.

Phase-sensitive amplifiers (PSAs) are well recognized to be able to realize noiseless amplification and have attracted much attention recently [1]. Particularly, a frequency nondegenerate PSA (signal and idler frequencies are different) has the potential to obtain broadband low-noise amplification, which is of importance for a wide range of applications [2]. The noise performance of a nondegenerate PSA has been studied both theoretically [3,4] and experimentally [5,6]. However, all the previous studies focused on the case where the input signal and idler powers are equal, and a −3 dB NF can be expected when considering signal or idler channel only [3,4]. In fact, a nondegenerate PSA provides a new degree of freedom—the input power ratio between signal and idler—compared with its degenerate counterpart. Thus it is useful for both understanding and optimizing the nondegenerate phase-sensitive amplification to investigate the noise performance with unequalized input powers.

Under the undepleted pump approximation, the input–output relation of a nondegenerate PSA is [3,4,6]

$$\begin{bmatrix} A_s \\ A_i^* \end{bmatrix} = \begin{bmatrix} \mu & \nu \\ \nu^* & \mu^* \end{bmatrix} \begin{bmatrix} A_{s0} + \delta A_s \\ A_{i0}^* + \delta A_i^* \end{bmatrix}, \tag{1}$$

where $A$ is the complex amplitude, subscripts $s$ and $i$ denote signal and idler waves, respectively, $A_{s0}$ and $A_{i0}$ are the input signal and idler amplitudes, respectively, superscript $*$ is the conjugation operation, and $\mu$ and $\nu$ are the complex transfer coefficients, which satisfy the auxiliary equation $|\mu|^2 - |\nu|^2 = 1$. $\delta A_s$ and $\delta A_i$ denote the uncorrelated vacuum noise fields at signal and idler frequencies. The statistics of the vacuum noise is assumed to be complex Gaussian. In this Letter, we only consider the copolarized pump–signal–idler case with optimal relative phase; thus, the maximal phase-sensitive signal/idler gain will be

$$\begin{aligned} G_{\mathrm{PSA},s} &= (\sqrt{GP_{s0}} + \sqrt{(G-1)P_{i0}})^2/P_{s0}, \\ G_{\mathrm{PSA},i} &= (\sqrt{GP_{i0}} + \sqrt{(G-1)P_{s0}})^2/P_{i0}, \end{aligned} \tag{2}$$

where $G = |\mu|^2$ is the phase-insensitive gain and $P_{s0} = |A_{s0}|^2$ and $P_{i0} = |A_{i0}|^2$ are the input signal and idler powers. According to Eq. (2), the signal and idler output powers are almost equal in the high-gain region. Because signal and idler are at different wavelengths, a straightforward NF definition is to consider each wave individually [3–5]. In this case, the separate NF can be obtained from Eq. (1) as [4]

$$NF_k = SNR_{\mathrm{in},k}/SNR_{\mathrm{out},k} = (2G-1)/G_{\mathrm{PSA},k}, \tag{3}$$

where $SNR_{\mathrm{in/out}}$ denotes the signal-to-noise ratio for direct detection at the input or output of the amplifier, and subscript $k$ represents the signal or idler wave. Based on this definition, a −3 dB separate signal/idler NF can be expected at high gain when the input powers are equal, because the phase-sensitive gain will be about 6 dB higher than the phase-insensitive gain; however, it becomes 0 dB at unity gain [4]. Note that, for $G \gg 1$, $G_{\mathrm{PSA},s} \approx G_{\mathrm{PSA},i} \times P_{i0}/P_{s0}$ and $NF_s \approx NF_i \times P_{s0}/P_{i0}$. On the other hand, the NF of a nondegenerate PSA can be defined in a combined manner, which considers signal and idler waves together as the amplifier input and output [3,4,7]. The $SNR_{\mathrm{in/out}}$ can be measured by simultaneously detecting signal and idler waves with a photodetector (PD) at the input and output (assuming that the PD is sensitive to both signal and idler wavelengths, while its electrical bandwidth is much smaller than the frequency separation between the two waves, and thus their beating components will not be detected) [7]. The combined NF can be obtained by neglecting the spontaneous–spontaneous noise contribution in the total photocurrent of the signal and idler waves:

$$NF_c = \frac{(P_{s0}+P_{i0})[(\sqrt{GP_s} + \sqrt{(G-1)P_i})^2 + (\sqrt{GP_i} + \sqrt{(G-1)P_s})^2]}{(P_s+P_i)^2}, \tag{4}$$

 

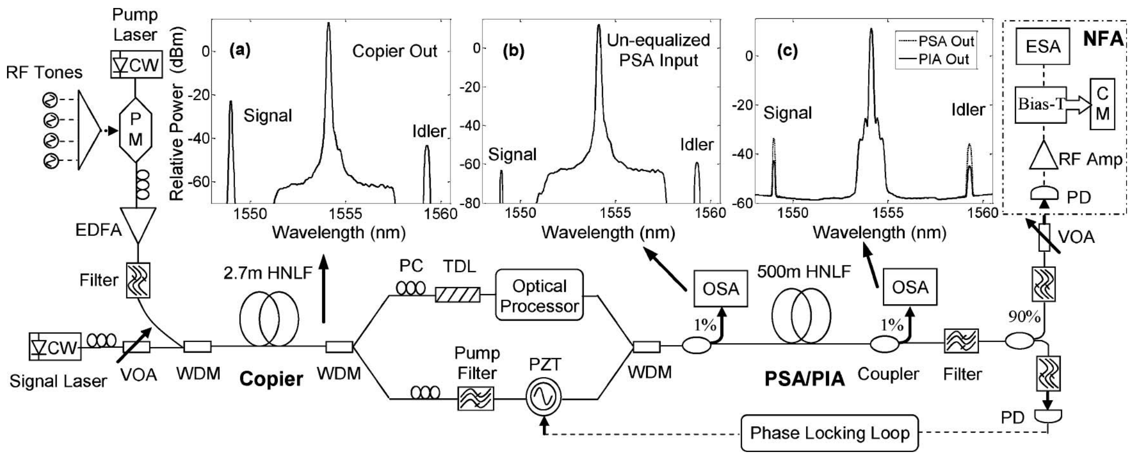


Fig. 1. Experimental setup and typical optical spectra at (a) copier output, (b) PSA input (with 6 dB idler-to-signal ratio), (c) PSA (with 6 dB idler-to-signal ratio), and PIA (with the same signal input power) outputs. PC, polarization controller; VOA, variable optical attenuator; TDL, tunable delay line; PM, phase modulator; PD, photodetector; CM, current meter; ESA, electrical spectrum analyzer; NFA, noise–figure analyzer.

where $P_s = P_{s0} G_{\mathrm{PSA},s}$ and $P_i = P_{i0} G_{\mathrm{PSA},i}$ are the output signal and idler powers. According to Eq. (4), when the signal and idler input powers are equal, the combined NF will be 0 dB, independent of the gain. It is consistent with the prediction of the noiseless amplification [8]. When the idler is absent at the input, the combined NF then becomes $2 - 1/(2G - 1)^2$, which for $G \gg 1$ approaches the well-known "3 dB" NF limit of a phase-insensitive amplifier (PIA) [3,4]. Moreover, in the high-gain region, one has $\sqrt{G} \approx \sqrt{G-1}$, and then Eq. (4) can be reduced to

$$NF_c \approx NF_s + NF_i \approx NF_s \cdot \frac{P_{s0} + P_{i0}}{P_{s0}} \approx NF_i \cdot \frac{P_{s0} + P_{i0}}{P_{i0}}, \tag{5}$$

which means that the combined NF approximately equals the summation of the separate signal and idler NFs.

The nondegenerate PSA characterized in this paper is based on a copier–PSA structure, which utilizes a parametric PIA-based copier, followed by the PSA stage [9]. In this scheme, an automatically phase- and frequency-locked signal–idler–pump triplet will be created by the copier; however, the copier also adds excess noise to both signal and idler waves, which should be subtracted for the PSA NF measurement [6]. This subtraction is further complicated by the fact that the copier generates an unwanted correlation between the signal and idler noises, whereas for NF measurement, the signal and the idler noises at the PSA input should be uncorrelated [3,4]. In practice, the signal and idler noises can be decorrelated after experiencing sufficient loss [6,10].

The experimental setup is shown in Fig. 1. A cw signal (1549 nm) and phase-modulated pump (1554.4 nm wavelength and 3.2 W launched power) are combined via a WDM coupler, and then input into the copier. The copier consists of 2.7 m of highly nonlinear fiber (HNLF), and zero-dispersion wavelength, nonlinear coefficient, and dispersion slope are 1553.6 nm, $10\ \mathrm{W^{-1} km^{-1}}$, and $0.02\ \mathrm{ps/nm^2 \cdot km}$, respectively), which provides less than 0.1 dB parametric gain, and thus the copier excess noise is negligible. Because of this very small copier gain, an asymmetric signal–idler output with a 19 dB power difference is created, as shown in Fig. 1, inset (a). The pump is phase-modulated by four discrete radio frequency tones, which are approximately 100, 300, 900, and 2700 MHz, to suppress the stimulated Brillouin scattering in the PSA stage. After the copier stage, an optical processor (OP) is used to independently adjust the power of the signal and idler. Because of the power handling limitation of the OP, the pump wave is separated via another WDM coupler. Through the OP, the idler-to-signal power ratio

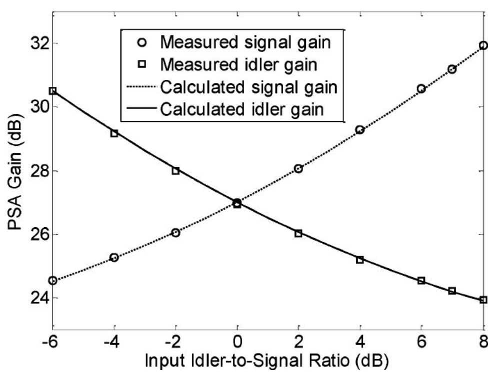


Fig. 2. Measured and calculated PSA gain as a function of the input idler-to-signal-power ratio.

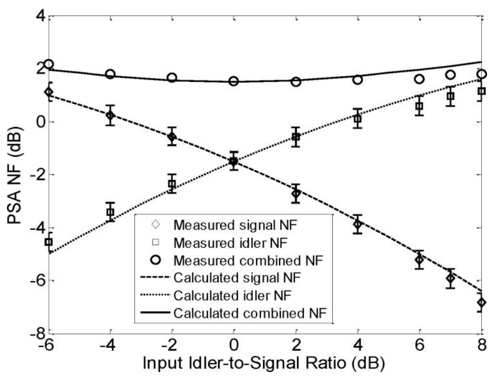


Fig. 3. Measured and calculated separate/combined NF versus input idler-to-signal-power ratio. The PSA input idler power is −36 dBm.

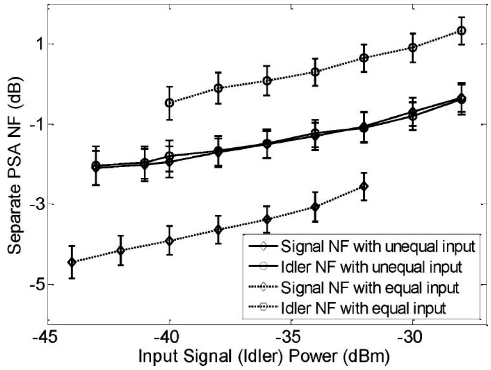


Fig. 4. Measured signal and idler NFs versus input signal/idler power under equal-input and unequal-input (with 4 dB idler-to-signal ratio) conditions.

after the copier can be easily adjusted, as shown in inset (b), and the amplification can be switched between PSA and PIA modes by simply turning the idler on and off. Subsequently, pump, signal, and idler waves are combined again to input to the second HNLF to realize phase-sensitive amplification. The PSA consists of 500 m of HNLF (zero dispersion wavelength, nonlinear coefficient, and dispersion slope are 1552 nm, $11.8\ \mathrm{W^{-1}km^{-1}}$, and $0.02\ \mathrm{ps/nm^2 \cdot km}$, respectively). The pump power launched into the PSA is about 1.1 W, which results in 26.5 dB PSA gain at 1549 nm signal wavelength. To achieve a maximal and stable PSA output, a piezoelectric-transducer-based optical phase-locked loop is implemented to compensate the slow phase drift induced by temperature variations and acoustic vibrations between the two branches of the interferometerlike structure. Finally, the amplified signal wave is filtered out for NF measurement based on the relative-intensity-noise (RIN) subtraction method used in [6], because the input RIN (arising from the input signal laser before the copier) will experience the same PSA gain as the signal (or idler) does. In our experiments, the total loss that the signal experiences between the copier and the PSA is larger than 20 dB, which will almost completely decorrelate the signal and idler noise and satisfy the requirement of PSA NF measurements. Moreover, the PSA is operated in the linear regime, i.e., gain saturation does not occur.

In inset (c) of Fig. 1, the output optical spectra in both PSA (with 6 dB higher idler power) and PIA modes are compared at the same signal input power. It can be observed that the output signal and idler powers are almost equal in the PSA case, even with unequalized inputs, and the signal will have an about 10 dB excess gain over the PIA. In Fig. 2, we have measured both signal and idler gains versus idler-to-signal ratio, which agree well with the calculated results based on Eq. (2). These phenomena clearly show that a nondegenerate PSA tends to equalize the output powers by providing more gain for the weaker input wave, due to the highly correlated signal and idler light. In Fig. 3, the separate signal and idler NFs are also measured versus idler-to-signal-ratio and the combined NF is obtained by using Eq. (5). The theoretical NFs are also calculated according to Eqs. (3) and (4), and both signal and idler NFs are upshifted by 1.5 dB (as a fitting parameter) to account for the spontaneous Raman scattering from thermal phonons and the distributed loss of the PSA HNLF [11]. Because the signal/idler wavelength and the phase-insensitive gain ($G$) are fixed, this excess noise should be constant for both signal and idler. The experimental results agree well with the theory; they clearly show that the noise performance of the lower-input wave will be improved, while the higher-input one will be degraded. It can be found that the signal NF is even lower than −3 dB (−7 dB) at an 8 dB idler-to-signal ratio, while the combined NF is always above 0 dB, and its lowest value of $(1.5 \pm 0.35)$ dB can be obtained by launching equalized signal and idler inputs. In this sense, the combined NF definition is more general and physically consistent. Finally, the separate signal and idler NFs versus input signal (or idler) power are shown in Fig. 4 under equalized and unequalized input conditions. One can see that the signal and idler NF curves are almost identical at the equal-input condition, but deviate at the unequal-input case. The reason why the NF curves increase with the increased input signal power is pump-transferred noise [12] and residual acoustic noise caused by the phase-locked loop [13]. This result further confirms that the noise performance of the input wave with lower power will be improved. This unique characteristic might be helpful in some applications that require high SNR performance or detecting very low power at specific wavelengths.

The research leading to these results has received funding from the European Commission Seventh Framework Programme FP/2007–2013 under grant agreement 224 547 (STREP PHASORS). The copier and PSA HNLFs were provided by Sumitomo and OFS, respectively. The authors would like to thank A. Bogris and C. J. McKinstrie for fruitful discussions.

## References

1. P. A. Andrekson, C. Lundström, and Z. Tong, in *ECOC 2010*, (IEEE, 2010), paper We.6.E1.
2. M. Vasilyev, in *Frontiers in Optics* (Optical Society of America, 2010), paper FThB1.
3. C. J. McKinstrie, M. Yu, M. G. Raymer, and S. Radic, Opt. Express **13**, 4986 (2005).
4. M. V. Vasilyev, Opt. Express **13**, 7563 (2005).
5. O. K. Lim, V. S. Grigoryan, M. Shin, and P. Kumar, in *Optical Fiber Communication Conference (OFC)* (Optical Society of America, 2008), paper OML3.
6. Z. Tong, A. Bogris, C. Lundström, C. J. McKinstrie, M. Vasilyev, M. Karlsson, and P. A. Andrekson, Opt. Express **18**, 14820 (2010).
7. P. L. Voss, K. G. Köprülü, and P. Kumar, J. Opt. Soc. Am. B **23**, 598 (2006).
8. H. P. Yuen, Phys. Rev. A **13**, 2226 (1976).
9. R. Tang, L. Jacob, P. S. Devgan, V. S. Grigoryan, P. Kumar, and M. Vasilyev, Opt. Express **13**, 10483 (2005).
10. C. J. McKinstrie, M. Karlsson, and Z. Tong, Opt. Express **18**, 19792 (2010).
11. R. Tang, P. L. Voss, J. Lasri, P. Devgan, and P. Kumar, Opt. Lett. **29**, 2372 (2004).
12. Z. Tong, A. Bogris, M. Karlsson, and P. A. Andrekson, Opt. Express **18**, 2884 (2010).
13. A. Bogris, D. Syvridis, and C. Efstathiou, J. Lightwave Technol. **28**, 1209 (2010).